The HKU Scholars Hub   The University of Hong Kong   香港大學學術庫

Title	Phase transformation behaviour of porous NiTi alloys fabricated by capsule-free hot isostatic pressing
Author(s)	Wu, SL; Liu, XM; Chu, PK; Chung, CY; Chu, SL; Yeung, KWK
Citation	The 1st International Symposium on Functional Materials, Kuala Lumpur, Malaysia, 6-8 December 2005, p. 64-70
Issued Date	2005
URL	http://hdl.handle.net/10722/103622
Rights	This work is licensed under a Creative Commons Attribution-NonCommercial-NoDerivatives 4.0 International License.

Phase transformation behaviour of porous NiTi alloys fabricated by capsule-free hot isostatic pressing

S.L. Wu [a], X.M. Liu [a], P.K. Chu [a], C.Y. Chung [a,*], C.L. Chu [b], K.W.K. Yeung [c]

a Department of Physics &Materials Science, City University of Hong Kong, Kowloon, Hong Kong
b Department of Materials Science and Engineering, Southeast University, Nanjin 210018,PR China
c Division of Spine Surgery, Department of Orthopaedics and Traumatology, The University of Hong Kong, Pokfulam, Hong Kong

*Corresponding Author: C.Y. Chung; Tel. :(852) 2788-7835; Fax :(852) 2788-7830
E-mail address: appchung@cityu.edu.hk

Keywords: Shape Memory Alloy, Porous NiTi; Differential scanning calorimetry; Hot isostatic pressing

Abstract. Differential scanning calorimetry (DSC) was used to characterize the phase transformation behaviour of porous $Ni_{50}Ti_{50}$ alloys fabricated by capsule-free hot isostatic pressing (CF-HIP) with different cold compaction pressures. Experimental results reveal that a multi-stage martensitic transformation (MST) exists in the sintered porous NiTi alloys on cooling while the reverse transformation upon heating is either a single or two-stage phase transformation. The DSC thermal analysis indicates that the cold compaction pressure has great effect on the subsequent transformation temperatures. Generally, the phase transformation temperatures of porous NiTi alloys with lower cold compaction pressure are higher than those compacted with higher pressure. With increase in the annealing time, the transformation temperatures increase quickly when the cold compaction pressure was 150MPa. On the other hand, the transformation temperatures change only slightly when the cold compaction pressure was varied from 300MPa to 400MPa. These phenomena can be attributed to the combined effect of larger plastic deformation with higher dislocations density produced by cold compaction and the precipitation of the second phase in the porous NiTi alloys.

Introduction

Recently, one of the focuses of orthopaedics and biomedical engineers is the development of porous nickel-titanium (NiTi) shape memory alloys (SMAs) for orthopedic implants. Porous NiTi SMA is attractive because it is a promising biomaterials for hard tissue reconstruction and artificial bone graft due to the unique shape memory effect (SME) and superelasticity (SE). Various methods have been developed for the fabrication of porous NiTi alloys, such as elemental powder sintering (EPS) in argon [1], self-propagating high temperature synthesis (SHS) [2,3], spark plasma sintering (SPS) and hot isostatic pressing (HIP) [4,5].

It is well accepted that the SME and SE of NiTi SMAs depend critically on the reversibility of the martensitic transformation. In the last decades, the martensitic transformation behavior of dense NiTi alloys had been extensively studied using differential scanning calorimetry (DSC) [6, 7]. For equiatomic dense NiTi alloys, the martensitic transformation usually shows a one step

transformation from the high temperature parent B2 phase to the low temperature monoclinic martensite phase B19′. Two steps or multi-stage martensitic transformation (MST) can also occur in dense NiTi alloys after certain thermal or mechanical treatments which can be described as B2→R (intermediate trigonal martensite), R→B19′, or B2→B19′. In the case of porous NiTi alloys, Chu and Li [8, 9] found that martensitic transformation in the porous NiTi alloys fabricated by SHS might exhibit one step or two stages transformation. In this investigation, a three-stage MST was found in porous NiTi alloys prepared by CF-HIP. The transformation behavior will be discussed correlating the effect of cold compaction pressure and the annealing time on the MST behavior in the porous NiTi alloys fabricated by CF-HIP.

Experimental procedure

CF-HIP sintering process was employed to fabricate the porous equiatomic NiTi SMA. Pure titanium and nickel powders with particle sizes of 50-75µm (purity > 99.5%) and 4-7 µm (purity > 99.9%) respectively were weighed with a precision of ±0.1 mg and put into a stainless steel can together with some stainless steel balls. The powder to ball ratio was 1:2 by weight. Before ball milling, argon gas was purged into the stainless steel can with powder mixture for 2 hrs in order to minimize the oxidation of powders during mixing. The mixtures were mixed for 12 hrs by ball mill with a speed of 100 rpm. Secondly, the mixed powders were pressed into green compacts in a steel mold with a diameter of 16mm using a hydraulic press at cold compaction pressures of 150MPa, 200MPa, 300MPa and 400MPa. The green compacts were put into capsule-free stainless steel canisters and reactive sintered in the HIP chamber. The HIP chamber was vacuum purged and backfilled with 99.995% high purity argon gas before increasing the HIP pressure to 100MPa. The temperature of the HIP chamber was then increased. The argon pressure and temperature reached 150 MPa and 1050 ^{0}C respectively at the same time. The high pressure and temperature were kept for 3hrs allowing sufficient solid state diffusion of the nickel and titanium atoms. It is believed that under high pressure, the Argon gas adhering on the surface of the internal pores will diffuse out and form pores. These pores will expand and help to form "spherical" pores, which is favorable for the formation of porous structure with lower stress concentration around the pores.

After HIPping, the porous NiTi SMA were annealed at 450 ^{0}C in tube furnace with continuous flow of 1 atm 99.995% high purity argon for 0.5hr, 1hr and 2hrs followed by quenching in ice water. The transformation behavior and characteristic temperature were determined using a DSC thermal analyzer (TA 2910 Instrument) with the specimen weight between 10 and 20 mg. In the DSC thermal analysis, specimens were heated up to 100 ^{0}C and kept isothermal for 2 min to establish thermal equilibrium, then cooled down to -50 ^{0}C, and also kept isothermal for 2 min and then ramped back to 100 ^{0}C again. All heating and cooling rates were kept at ±5 ^{0}C /min. The porous structure of the porous specimens was analyzed using scanning electron microscope (SEM JSM5200).

Results and discussions

Fig.1 shows the general morphology of porous NiTi fabricated by CF-HIP. It can be found that the porous NiTi alloys have obvious three-dimensionally interconnected porous structure and the pores size was in the range of 100 – 600 µm, which is suitable for tissue integration [10].

DSC results of the porous NiTi SMAs from different green compacts are shown in Figs. 2 to 5. It is obvious that a three-stage MST occurred upon cooling while the corresponding reverse transformation is either single step or two-steps. It is known that R-phase will form prior to the formation of B19′ which is due to the presence of secondary phase such as metastable Ni_4Ti_3 precipitates and dislocation substructures [7, 11]. This infers that the first peak in Figs. 2 to 5 on

cooling corresponds to the B2→R transformation. The second peak represents the R→B19′ transformation. The third peak in the cooling curve at lower temperature (shown in Figs 2 to 5 (a)), can be attributed to the transformation of the remaining R-phase to B19′. The above result is in good agreement with the explanation proposed by Carroll et al. [11]. They believed that the transformation in the second step is not completely due to the obstacle of the dislocation. It is necessary to provide sufficient energy for the further transformation to overcome such obstacle. When the temperature is lowered, the B19′ phase will nucleate in the remaining R-phase which possess more driving force so that it can penetrate the obstacles. As for the reverse transformation, according to Su et al. [12], the peak 1′ and 2′ in the heating curves correspond to B19′ →R→ B2 and B19′ →B2, respectively.

It is worthy to mention that the phase transformation behavior of porous NiTi alloy prepared by CF-HIP is different from those of porous NiTi alloy fabricated by SHS. Chu et al. [8] reported that no MST has occurred in the porous NiTi alloy prepared by SHS. The discrepancy is because the high cold compaction pressure with subsequent HIPping pressure in our work can provide a much stronger initial stress field. This initial stress combined with the coherency stress fields around metastable Ni_4Ti_3 precipitates, as proposed by Bataillard et al. [13], favors the formation of a MST behavior. After the first step of the MST (peak 1 on cooling curve), R-phase nucleating at the interface between Ni_4Ti_3 precipitates and B2 grows into the matrix. In the second stage, the R-phase transforms into B19′, but the transformation is not complete because the initial stress and coherency stress around Ni_4Ti_3 precipitates can block the growth of the B19′ phase in the stressed region. When the temperature is lowered, B19′ nucleates and grows in volume away from the higher stress region and the precipitates-free region. This corresponds to the third peak on cooling curve (R→B19′).

As shown in Figs 2 to 5, the onset of the first exothermic peak in the high temperature side corresponds to the start temperature (Rs) of the transformation to the low temperature phase (B2→R) while the onset in the lower temperature of the first endothermic peak corresponds to the start temperature (As) of the reverse transformation to the high temperature phase (B19′ →B2). Generally, it can be found from Table 1 that the Rs and the exothermic peak temperatures (peak 1 and 2) of porous NiTi with lower cold compaction pressure are higher than those of porous samples with higher cold pressure. It suggests that exothermic phase transformation is easier to occur in porous NiTi alloys with lower cold pressures such as 150MPa and 200MPa while it is difficult in samples made by higher cold compaction pressure such as 300MPa and 400MPa. As mentioned before, a higher cold pressure exerts a higher initial stress, which increases the density of dislocation and also strengthens the coherency stress field around Ni_4Ti_3 precipitates. Therefore, each exothermic stage of MST in porous NiTi alloy with high cold pressure cannot go through unless sufficient driving force is built up. We also note that the As of the porous NiTi alloys with lower cold compaction pressures is higher than those with higher cold compaction pressures. It means that endothermic phase transformation (B19′ →B2) in samples with lower cold compaction pressures is more difficult to occur relative to specimens with higher cold compaction pressures. This is possibly due to the easier exothermic phase transformation occurring in specimens with lower compaction pressures, which results in a great deal of B19′ twin crystals and more dislocations. Therefore, higher temperature is required to activate it's the corresponding reverse transformation (B19′ →B2).

It is important to note that the annealing time can significantly influence the transformation behavior of porous NiTi alloy with lower cold compaction pressure. For example, for porous NiTi alloy with a compaction pressure of 150 MPa, the Rs and exothermic peak (peak 1 and 2) increase fairly quickly as the annealing time increases (shown in Fig.2 (a)). It is also obvious that the ΔT (temperature difference between peak 2 and 3) increases sharply as the annealing time increases (shown in Fig.2 (a)). However, for porous NiTi alloy with higher cold compaction pressures, the

annealing time can only change the transformation temperatures slightly. And the ΔT increases little as the annealing time increases (shown in Figs. 4(a) and 5(a)). According to Chrobak et al. [14], it can be concluded that under a lower initial stress exerted by a lower compaction pressure, with increasing of the annealing time, the dislocations can easily bend more toward the precipitates, resulting in an increase in the high dislocation volume. On the other hand, some internal residual stress can be reduced by increasing the annealing time. Therefore, the first step transformation $(B2 \rightarrow R)$ occurs easily while it is necessary to get more energy to start the second step transformation $(R \rightarrow B19')$ and the third transformation (remaining $R \rightarrow B19'$). It can be found from Fig. 3 (a) that the 2hrs cooling curve of porous NiTi alloy with a cold pressure of 200MPa is quite different with peak 2 merged with peak 3. According to the argument of [14], two separate transformations $R \rightarrow B19'$ occurs in different regions with different density of precipitates in the MST process. We speculate that the density of precipitates in the porous sample possibly becomes uniform as the annealing time is lengthened from 0.5hr to 2hrs, resulting in the merging of two separate transformations.

Conclusion

A three-stage MST occurs in the porous NiTi SMA fabricated by CF-HIP in this work. The first and second exothermic peak in the cooling curve correspond to the transformations $B2 \rightarrow R$ and $R \rightarrow B19'$, respectively. The presence of the third exothermic peak, which should correspond to the transformation of remaining R to $B19'$, is due to the fact that the high dislocation density caused by higher cold compaction pressure and the subsequent higher argon pressure in the HIPping process which hinder the process of the second step transformation. The cold pressures substantially affect the phase transformation behaviors of the sintered porous NiTi alloys produced by CF-HIP. Generally, with lower cold compaction pressures, the transformation temperatures of porous NiTi SMA are higher than those with higher cold compaction pressure. Besides, with lower cold compaction pressures, the transformation temperatures will increase fairly quickly as the annealing time increases while the change is little with longer annealing time under higher cold compaction pressures. This is because under a lower initial stress exerted by a lower cold compaction pressure, with increase in the annealing time, the dislocations suppressed by initial and coherency stress fields around the secondary particles can recover and accumulate relatively easier. We suggest that the three-stage MST behavior should be attributed to the combined effect of initial stress, high dislocations density produced by high cold compaction pressures and the precipitation of the second phase.

Acknowledgement

References

[1] B.Y. Li, L.J. Rong, Y.Y. Li, J. Mater. Res. 13 (1998) 2847.
[2] C.L. Chu, C.Y. Chung, P.H. Lin, S.D. Wang, Mater. Sci. Eng. A 366 (2004) 114.

[3] B.Y. Li, L.J. Rong, Y.Y. Li, V.E. Gjunter, Acta Mater. 48 (2000) 3895.

[4] Y. Zhao, M. Taya, Y. Kang, A. Kawasaki, Acta Mater. 53 (2005) 337.

[5] D.C. Lagoudas, P.B. Entchev, E.L. Vandygrift, in: Proceedings of SPIE, Smart structures and materials, 4333 (2001) 141.
[6] S.K. Wu, H.C. Lin, T.S. Chou, Acta Metall. Mater. 38 (1990) 95.

[7] J. Khalil Allafi, X. Ren, G. Eggeler, Acta Mater. 50 (2002) 793.

[8] C.L. Chu, C.Y. Chung, P.H. Lin, Mater. Sci. Eng. A 392 (2005)106.

[9] B.Y. Li, L.J. Rong, Y.Y. Li, V.E. Gjunter, Metall. Mater. Trans. A 31 (2000) 1867.

[10] D. Tadic, F. Beckmann, T. Donath, M. Epple, Materialwiss. Werkst. 35 (2004) 240.

[11] M.C. Carroll, Ch. Somsen, G. Eggeler, Scripta Mater. 50 (2004) 187.

[12] P.C. Su, S.K. Wu, Acta Mater. 52 (2004) 1117.

[13] L. Bataillard, J.E. Bidaux, R. Gotthardt, Philos. Mag. 78 (1998) 327.

[14] D. Chrobak, D. Stroz, H. Morawierc, Scripta Mater. 48 (2003) 571.

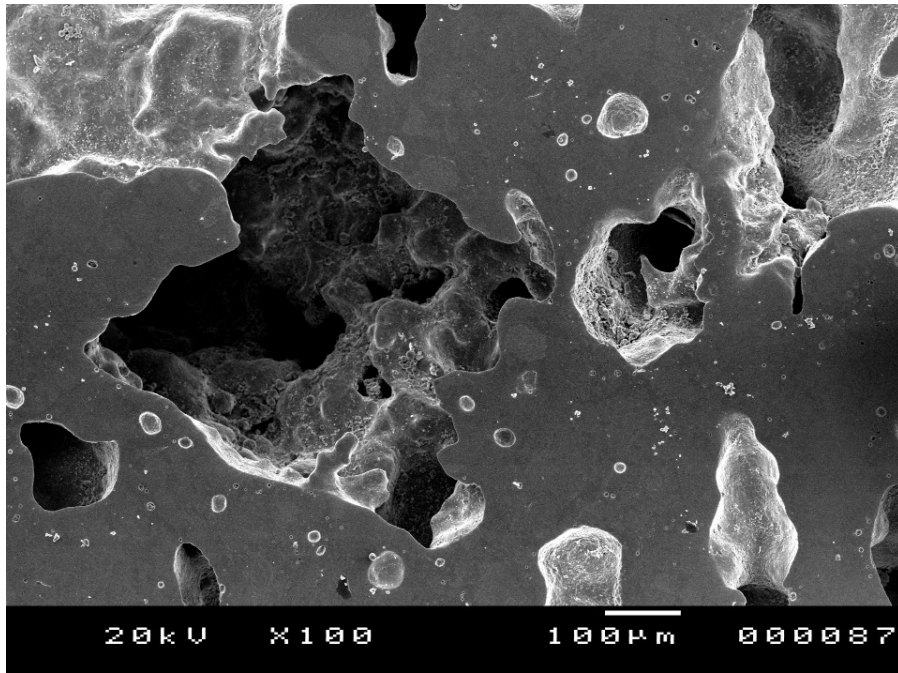**Figure Captions**

Figure 1: SEM micrograph of porous NiTi SMA by CF-HIP

Figure 2: DSC cooling – heating curves for porous $Ni_{50}Ti_{50}$ SMA fabricated by CF-HIP from green compact at 150MPa (a) cooling and (b) heating..

Figure 3: DSC cooling – heating curves for porous $Ni_{50}Ti_{50}$ SMA fabricated by CF-HIP from green compact at 200MPa (a) cooling and (b) heating.

Figure 4: DSC cooling – heating curves for porous $Ni_{50}Ti_{50}$ SMA fabricated by CF-HIP from green compact at 300MPa (a) cooling and (b) heating.

Figure 5: DSC cooling – heating curves for porous $Ni_{50}Ti_{50}$ SMA fabricated by CF-HIP from green compact at 400MPa (a) cooling and (b) heating.

Table 1. Transformation temperature evolution as cold pressure and annealing time

| Samples		150MPa			200MPa			300MPa			400MPa		
Annealing time (hr)		0.5	1	2	0.5	1	2	0.5	1	2	0.5	1	2
Rs(℃)		30.6	34.7	41.6	29.1	33.1	39.9	29.0	30.8	31.9	28.2	29.7	31.3
As(℃)		13.0	20.1	26.9	8.9	13.1	19.4	7.8	12.8	18.1	6.6	10.9	15.4
Cooling peak(℃)	1st	22.7	26.3	33.8	21.8	24.1	27.7	18.7	21.1	23.5	18.0	21.1	23.1
	2nd	-13.8	-5.4	2.1	-17.1	-13.8	—	-21.2	-17.0	-12.4	-22.6	-17.2	-13.5
	3rd	-25.34	-26.8	-27.5	-29.8	-27.9	-26.0	-25.8	-25.8	-24.6	-28.4	-27.2	-26.1
heating peak(℃)	1st	—	—	—	15.1	17.6	18.6	—	—	—	—	—	—
	2nd	27.2	36.6	41.1	26.6	29.2	31.4	24.7	28.0	29.8	24.3	26.2	27.7

Fig.1 SEM micrograph of porous NiTi SMA by CF-HIP
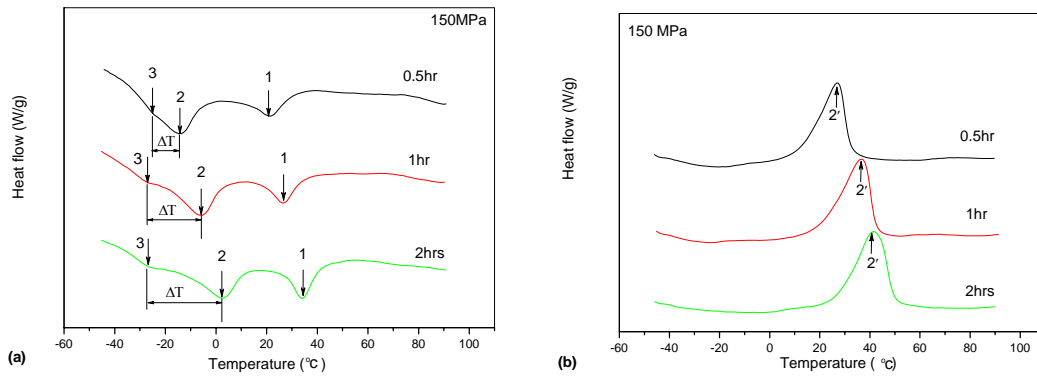
Fig. 2. DSC cooling – heating curves for porous $Ni_{50}Ti_{50}$ SMA fabricated by CF-HIP from green compact at 150MPa (a) cooling and (b) heating.
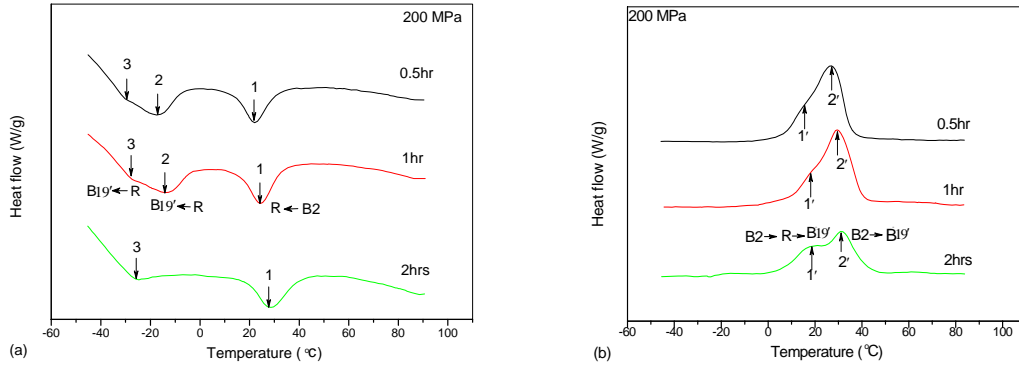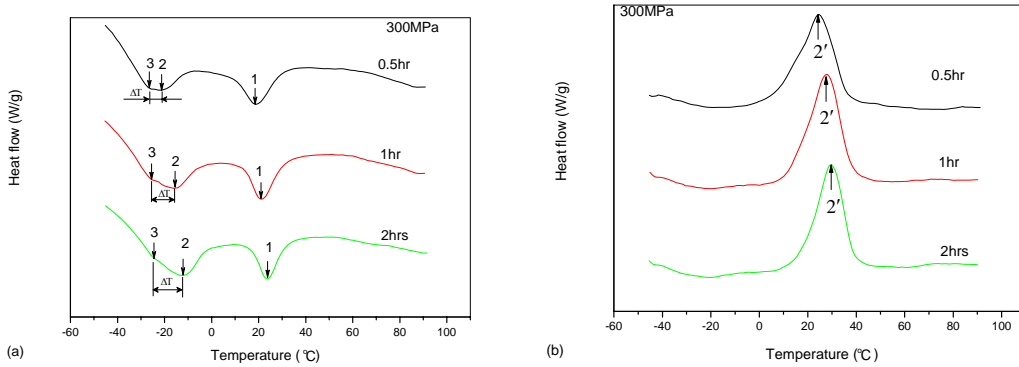
Fig. 3. DSC cooling – heating curves for porous Ni$_{50}$Ti$_{50}$ SMA fabricated by CF-HIP from green compact at 200MPa (a) cooling and (b) heating.

Fig. 4. DSC cooling – heating curves for porous Ni$_{50}$Ti$_{50}$ SMA fabricated by CF-HIP from green compact at 300MPa (a) cooling and (b) heating.
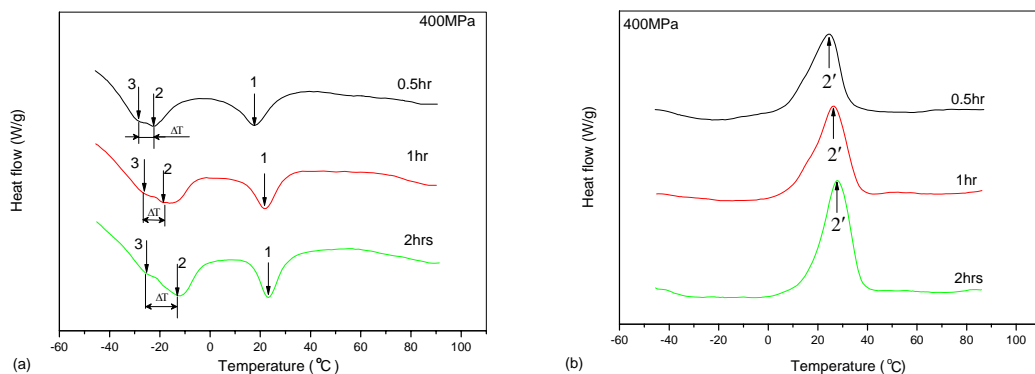

Fig. 5. DSC cooling – heating curves for porous Ni$_{50}$Ti$_{50}$ SMA fabricated by CF-HIP from green compact at 400MPa (a) cooling and (b) heating.